

Supplementary information

Photodynamic therapy using self-assembled nanogels comprising chlorin e6-bearing pullulan

Riku Kawasaki*,#, Reo Ohdake#, Keita Yamana, Takuro Eto, Kouta Sugikawa, and Atsushi Ikeda*

Program of Applied Chemistry, Graduate School of Advanced Science and Engineering, Hiroshima University, 1-4-1

Kagamiyama, Higashi Hiroshima, 739-8527, Japan

Table of Contents

Materials and Methods	S2-S5
Scheme S1 and Fig. S1	S6
Fig. S2	S7
Fig. S3 and S4	S8
Fig. S5 and S6	S9
Fig. S7 and S8	S10
Fig. S9, S10, and Table S1	S11
Scheme S2 and S11	S12
Fig. S12 and S13	S13
Fig. S14 and S15	S14
Fig. S16 and S17	S15
Fig. S18 and S19	S16
Fig. S20 and S21	S17
Fig. S22 and S23	S18
Fig. S24 and S25	S19

Materials and methods

Materials

Pullulan, pyrene, ethanol, dimethylsulfoxide anhydrous (DMSO), 4-dimethylaminopyridine (DMAP), and *N,N'*-dicyclohexylcarbodiimide (DCC) were purchased from FUJIFILM Wako Pure Chemical Corporation (Tokyo, Japan). Chlorin e6 and 9,10-anthracenediyl-bis(methylene)-dimalonic acid (ABDA) were purchased from Cayman Chemical Company (Michigan, USA) and Sigma Aldrich (USA), respectively. Human cervical cancer (HeLa), murine colon cancer (colon26), and murine melanoma (B16BL6) cells were maintained in Dulbecco's modified Eagle's medium (Thermo Fischer Science, Massachusetts, USA) containing 10% fetal bovine serum (Hyclone Laboratories Inc., Utah, USA) and 1% anti-anti (Nacalai Tesque; Kyoto, Japan). Cell Counting Kit-8 was purchased from Dojindo (Kumamoto, Japan).

Synthesis of chlorin e6-bearing pullulan

Pullulan was purified through dialysis (MWCO, 3.5 kDa) against water and lyophilized pullulan was used for synthesis. Pullulan (0.62 mmol) was dissolved in dry DMSO (3 mL) at 45 °C for 30 min, and DCC (0.015 mmol) was added to the resulting solution. Chlorin e6 (2.9, 7.2, or 14 µmol) was dissolved separately in dry DMSO. These two solutions were mixed and stirred at 45°C for 48 h. The resulting solution was placed in a dialysis membrane (MWCO, 3.5 kDa) and dialysis was performed against DMSO (1 d) and water (5 d). After lyophilization, samples were analyzed using ¹H-NMR (Varian 500 MHz, Agilent Technologies, Santa Clara, CA, USA) and Ultraviolet-Visible light absorption spectrum measurement (3600 UV-vis-NIR spectrometers; Shimadzu, Tokyo, Japan).

Nanogel formulation

Chlorin e6-bearing pullulan (1 mg) was stirred in milliQ (1 mL) overnight to dissolve all polymers completely. Then, sonication (Blanson Ultrasonics, USA) was performed on the resulting solution for 30 min with cooling. The formulation of the nanogel was confirmed by dynamic light scattering measurement (Zetasizer Nano ZS; Malvern, Malvern, UK) and transmission electron microscopy (JEM-1400 field emission electron microscope; JEOL Ltd., Tokyo, Japan).

Dynamic light scattering measurement

Hydrodynamic diameter (D_{hy}) and polydispersity index (PDI) of nanogels were measured using the Zetasizer Nano ZS, equipped with a He-Ne laser at 25°C (633 nm, 10 mW).

Transmission electron microscopy

Morphological evaluation of nanogels was performed using JEM-1400. Samples were cast on a hydrophilized Cu grid. After drying, the samples were stained with ammonium molybdate (1.5 wt%).

Field fractionation flow-multi angle light scattering (FFF-MALS)

Association number of polymers in each nanogel was evaluated using FFF-MALS. Measurements were performed

using an Eclipse DUALTEC separation system (Wyatt Technology Europe, Dernbach, Germany) connected to the Dawn HELEOS II multiangle light scattering (MALS) detector and Optilab rEX DSP differential refractive index (dRI) detector. The Eclipse 3 channel SC instrument was used for separation. Then, 30 μL nanogel dispersions were injected into an FFF separation channel (1 kDa polyether sulfone membrane; 250 μm spacer M type, SC-067). Processing and analysis of light scattering data and calculations for radius of gyration and molecular weight were performed using the ASTRA 7 software. Specific refractive index increment (dn/dc) values of the polymer were determined using the Optilab rEX DSP differential refractive index detector.

From the experimental D_{hy} ($2R_{hy}$) and M_w values, an average polymer density (Φ_H) within a Che6P nanogel was calculated according to

$$\Phi_H = (M_w/N_A)(4\pi R_H^3/3)^{-1} \quad (1)$$

where N_A is avogadro's number.

Association number of polymers within a Che6P nanogel (N_{Che6P}) was calculated according to

$$N_{\text{Che6P}} = M_w(\text{Che6P nanogel})/M_w(\text{pullulan}) \quad (2)$$

Here, M_w (pullulan) is 100,000.

Homogeneity of Che6P nanogel

To isolate free Che6P polymer, the dispersion of Che6P nanogel in water (1 $\text{mg}\cdot\text{mL}^{-1}$) was centrifuged using ultracentrifugation (120,000 $\times g$, 4 $^{\circ}\text{C}$, 90 min). The supernatant of the resulting solutions and dispersion of Che6P nanogels were mixed with sulfuric acid and 10% phenol solution. The resulting solutions were heated at 90 $^{\circ}\text{C}$ for 30 min. Afterward, the absorption spectra of the colored solution were measured by UV-Vis spectrometer. Here, unmodified pullulan was used to establish calibration curve.

Fluorescence-probe method using pyrene

Fluorescence spectra were recorded using a fluorescence spectrophotometer (F-2700; Hitachi Ltd., Tokyo, Japan). The stock solution of pyrene (1.0×10^{-3} M) in ethanol was added to a vial and the solvent was vaporized through flowing dried nitrogen gas to form a thin film of pyrene at the bottom of the vial. The nanogel dispersion was added to the vial and stirred overnight (approximately 18 h) at 25 $^{\circ}\text{C}$. The final concentration of pyrene was 1.0×10^{-6} M. Pyrene was excited at 339 nm.

Singlet oxygen species generation

Singlet oxygen species generated through photoirradiation were monitored by quenching of the anthracene derivative 9,10-anthracenediyi-bis(methylene)dimalonic acid (ABDA). The ABDA stock solution in DMSO was added to the nanogel dispersion in milliQ (nanogel, 100 $\mu\text{g}\cdot\text{mL}^{-1}$; ABDA, 2.5 μM ; DMSO, 1%). Oxygen was bubbled through the sample for 30 min before photoirradiation. Photoirradiation was performed using a Xenon lamp (SX-UID500X; Ushio Inc., Tokyo, Japan) equipped with a long-path filter with a cut-off at 620 nm and the filter was cooled with water. The power of the light used was 16 $\text{mW}\cdot\text{cm}^{-2}$.

Photodynamic activity against cancer cell lines

HeLa, colon26, or B16BL6 cells were seeded on 48-well plates at 1.75×10^4 cells/well and incubated overnight (approximately 18 h). Cells were exposed to various concentrations of nanogels in aqueous media for 24 h. After exchanging the medium, cells were irradiated with an optimal wavelength (>620 nm) of light for 30 min. Cells were additionally incubated for 24 h. Then, the cell counting kit was used to count cells. Absorbance at 450 nm was measured to determine cell viability.

Cellular uptake of nanogels (Flow cytometry)

HeLa, colon26, or B16BL6 cells were seeded on 12-well plates at 1.0×10^5 cells and incubated overnight (approximately 18 h). Cells were exposed to nanogels at $100 \mu\text{g}\cdot\text{mL}^{-1}$ for 24 h, collected using trypsin-EDTA, redispersed in sample buffer, and analyzed using flow cytometry (FACS Calibur; Becton Dickinson, New Jersey, USA).

Subcellular distribution of nanogel (Confocal laser scanning microscopy)

HeLa, colon26, or B16BL6 cells were seeded on glass-bottom dishes at 1.0×10^5 cells and incubated overnight (approximately 18 h). Cells were exposed to nanogels at $100 \mu\text{g}\cdot\text{mL}^{-1}$ for 24 h. Then, cells were washed with PBS and lysosomes were stained with commercially available Lysotracker Green (Thermo Fischer Scientific; Massachusetts, USA). Samples were observed using confocal laser scanning microscopy (LSM700; Carl Zeiss, Germany). Co-localization ratio (f) was calculated as following equation:

$$f = \text{Pixels(Che6P, colocalized)} / \text{Pixels (Che6P, total)}$$

Spheroid preparation

Colon26 cells were incubated in DMSO at $1.0 \times 10^7 \text{ cells}\cdot\text{mL}^{-1}$ with shaking (300 rpm) overnight (approximately 18 h). Spheroids were incubated for an additional 3 d on a 96-well plate. Spheroid volumes were calculated using the following equation (1). $V = \pi(\text{Long axis}) \times (\text{Short axis})^2 / 3 \square (1)$

Distribution of the nanogel in spheroids

Spheroids were exposed to $100 \mu\text{g}\cdot\text{mL}^{-1}$ nanogels for 24 h. Then, cells were washed with PBS. Nuclei were stained with DAPI after fixation with 4% glutaraldehyde and transparency processing with 0.1% PBST. Spheroids were observed using confocal laser scanning microscopy.

Spheroid growth inhibitory effects through photodynamic activity

Spheroids were exposed to $100 \mu\text{g}\cdot\text{mL}^{-1}$ nanogels for 24 h. Then, cells were washed with PBS. After exchanging medium, cells were light irradiated with optimal wavelength (>620 nm) for 30 min. Spheroidal volume was measured at each time point.

Establishment of tumor xenograft mice

To establish colon carcinoma xenograft model mice, suspension of colon26 cells in HBSS (5.0×10^5 cells/50 μ L) were subcutaneously injected toward Balb/c mice (Japan SLC, male, 4 weeks old, 20 g) in right femur and the mice were incubated for 14 days. The tumor-bearing mice were used for following biodistribution study and evaluation of anti-tumor efficacy. All animal experiments were performed in accordance with the Guidelines for care and use of laboratory animal of Hiroshima University and were approved by the ethics committee for animal welfare of Hiroshima University (accreditation, C21-2).

Biodistribution of Che6P nanogel

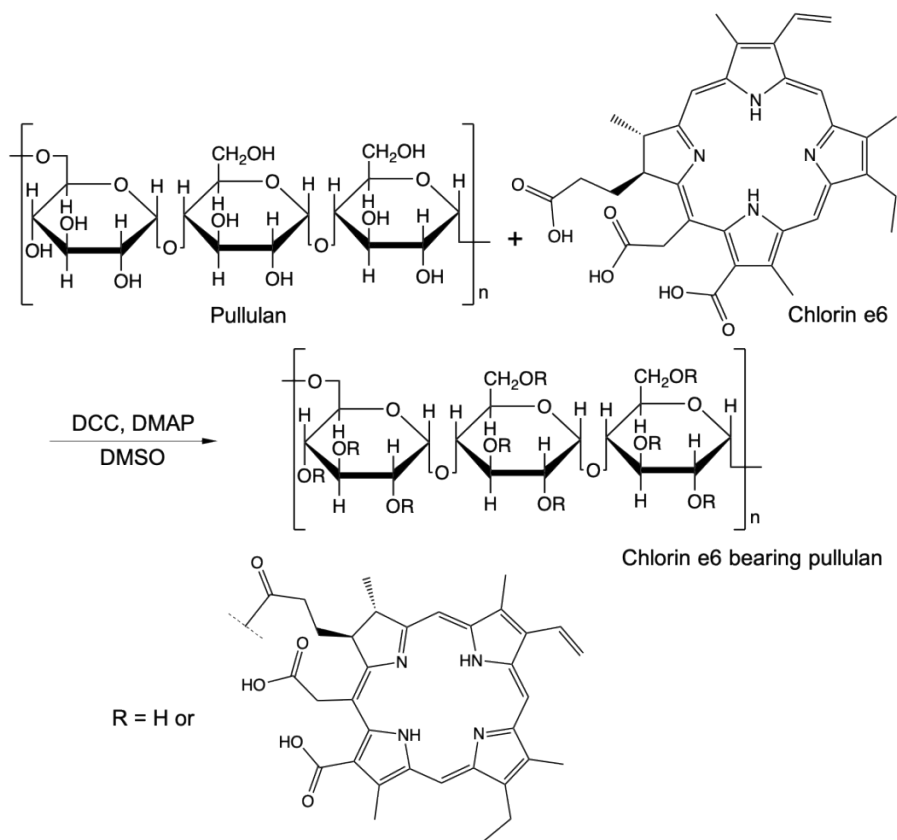
Dispersion of Che6P nanogel (1 mg•mL⁻¹, 100 μ L) were administered *via* tail vein injection toward tumor-bearing mice (n = 3). At each time point (1, 3, 6, and 24 h), the accumulation of Che6P nanogel was tracked by optical *in vivo* imaging system, Night OWL II (LB983, BERTHOLD TECHNOLOGIES, Germany). At 24 h, organs (heart, lung, liver, kidney, spleen, and tumor) were isolated and biodistribution was visualized by Night OWL II. In addition, intratumoral distribution of delivered Che6P nanogels was observed by confocal laser scanning microscopy. The cells were stained with Hoechst33342.

Photodynamic activity against tumor-bearing mice

Dispersion of Che6P nanogel (1 mg•mL⁻¹, 100 μ L) or solution of Photofrin (5 μ g•mL⁻¹, 100 μ L) were administered *via* tail vein injection toward tumor-bearing mice (n = 3) and the light irradiation was carried out for 1 h after 24 h. Afterward, tumor volume and body weight of the mice were measured at each time point and tumor volume was calculated by following formula. $V = \pi \times (\text{Long axis}) \times (\text{Short axis})^2 / 3$ (2)

Statistical analysis

All results are presented as mean \pm SD. Variance analysis was performed using Student's *t*-test (two-sided test). A significant *p*-value indicates a significant difference, where **p* < 0.05; ***p* < 0.1; and ****p* < 0.001. Analyses were performed using excel statistics.



Scheme S1. Synthesis of chlorin e6 bearing pullulan

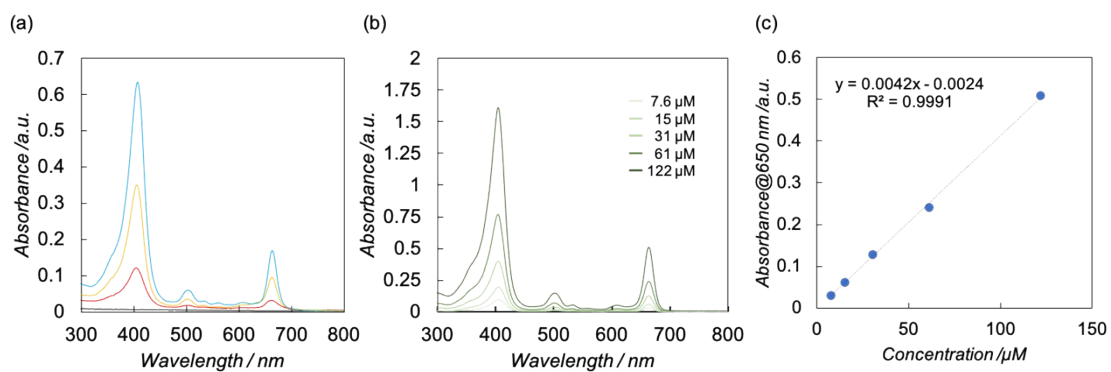


Fig. S1. (a) UV-Vis spectra of pullulan (black), Che6P-0.22 (red), Che6P-0.42 (yellow), and Che6P-0.72 (blue) in DMSO. The solution was prepared at 0.1 mg/mL. (b) UV-Vis spectra of chlorin e6 in DMSO (7.6, 15, 31, 61, and 122 μ M). (c) Calibration curve of chlorin e6 dissolved in DMSO for quantification of conjugated chlorin e6 with pullulan.

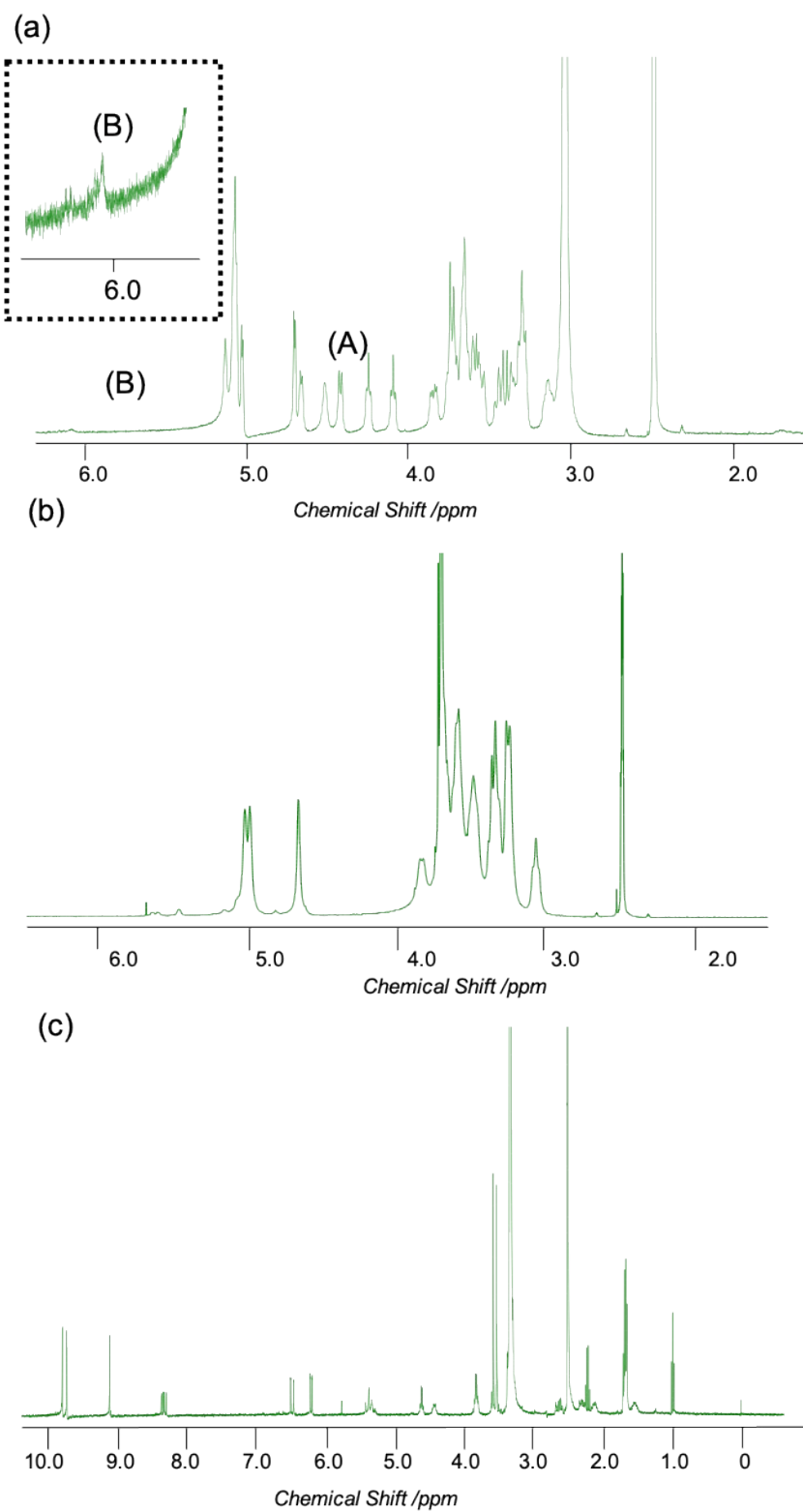


Fig. S2. ^1H -NMR spectra of (a) chlorin e6 bearing pullulan in mixture of d_6 -DMSO and D_2O (9:1). (A) anomeric proton in pullulan and (B) acrylic proton. (b) ^1H -NMR spectra of unmodified pullulan in mixture of d_6 -DMSO and D_2O (9:1). (c) ^1H -NMR spectra of chlorin e6 in d_6 -DMSO

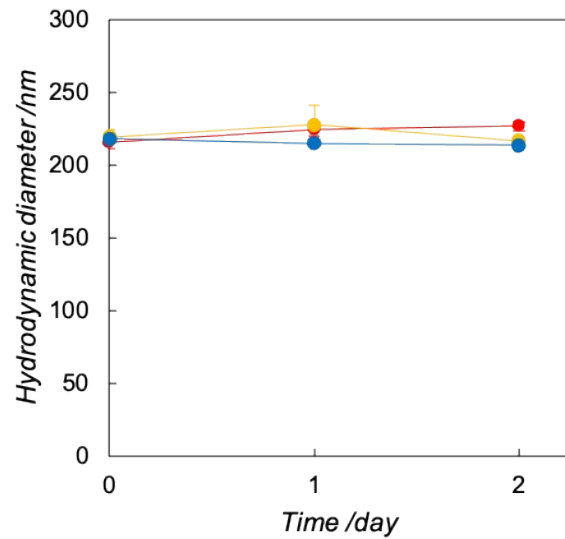


Fig. S3. Colloidal stability of the chlorin e6-bearing pullulan (Che6P) nanogel in aqueous media. (Che6P-0.22, red; Che6P-0.42, yellow; Che6P-0.72, blue).

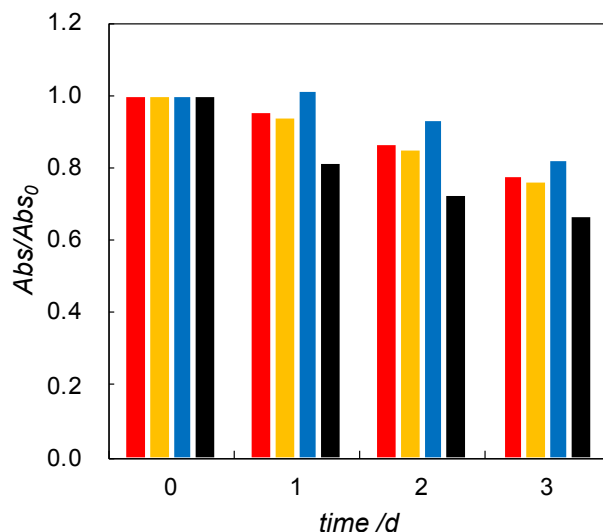


Fig. S4. Changes in absorption by chlorin e6-bearing pullulan (Che6P)-0.22 (red), Che6P-0.42 (yellow), Che6P-0.72 (blue), and chlorin e6 (black) at 660 nm.

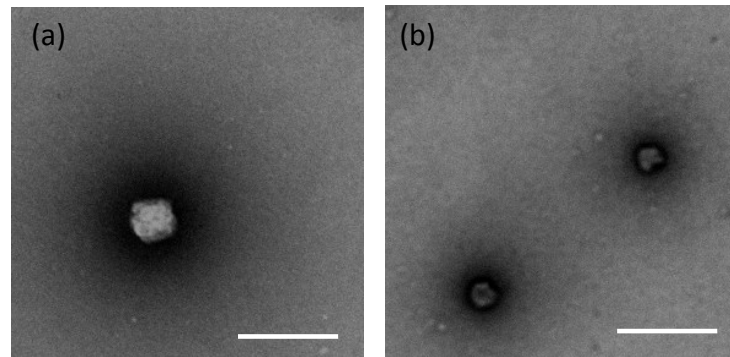


Fig. S5 Morphological observation of Che6P nanogels (Che6P-0.22, a; Che6P-0.42, b) using transmission electron microscopy. To visualize samples, negative staining was performed using 1.5% molybdenum. (Acceleration voltage, 100 keV) Scale bar represents 200 nm.

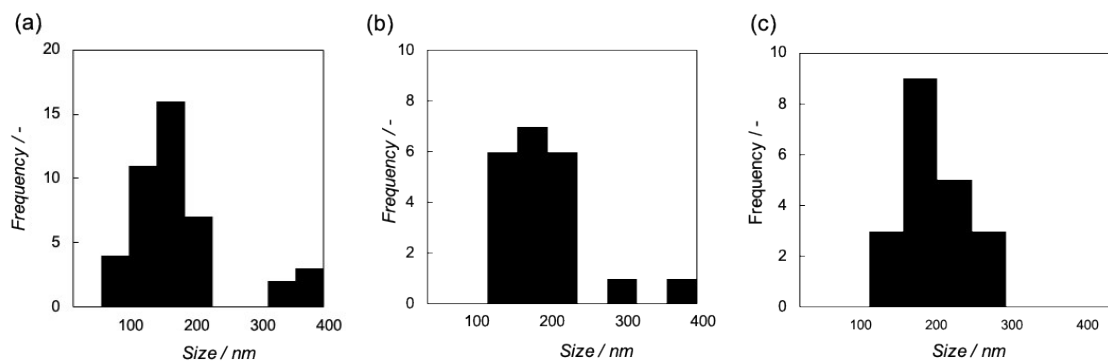


Fig. S6. Size distribution of chlorin e6-bearing pullulan (Che6P) nanogels (Che6P-0.22, a; Che6P-0.42, b; Che6P-0.72, c). Sizes were evaluated through ImageJ using more than 50 samples.

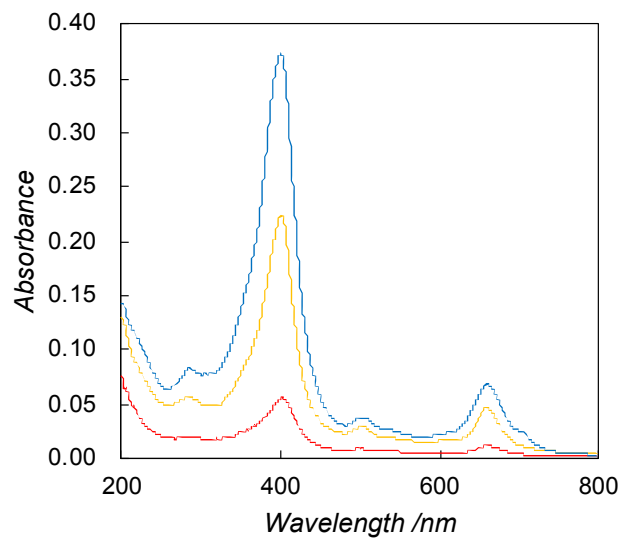


Fig. S7. UV-Vis spectra of chlorin e6-bearing pullulan (Che6P)-0.22 (red), Che6P-0.42 (yellow), and Che6P-0.72 (blue) in water. The dispersion was prepared at $0.1 \text{ mg} \cdot \text{mL}^{-1}$.

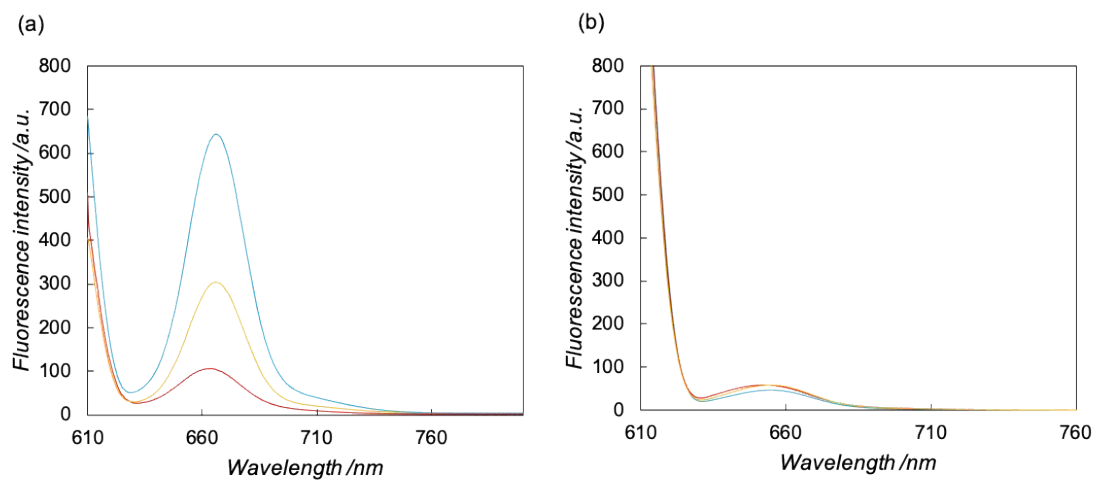


Fig. S8. Fluorescence spectra of chlorin e6-bearing pullulan (Che6P)-0.22 (red), Che6P-0.42 (yellow), and Che6P-0.72 (blue) in DMSO (a) and water (b). Dispersions of Che6P nanogels were prepared at $0.1 \text{ mg} \cdot \text{mL}^{-1}$.

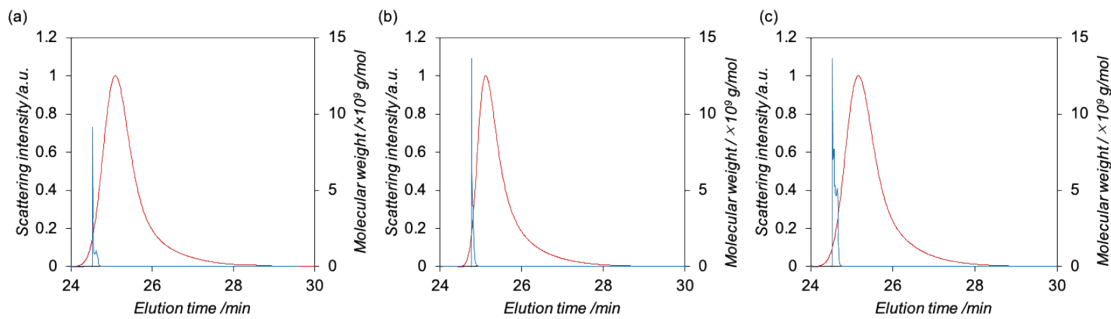


Fig. S9. Field flow fractionation-chromatogram of chlorin e6-bearing pullulan (Che6P) nanogels (a) Che6P-0.22, (b) Che6P-0.42, and (c) Che6P-0.72. Red curve and blue curve represent scattering intensity of polymer and molecular weight of the polymer, respectively.

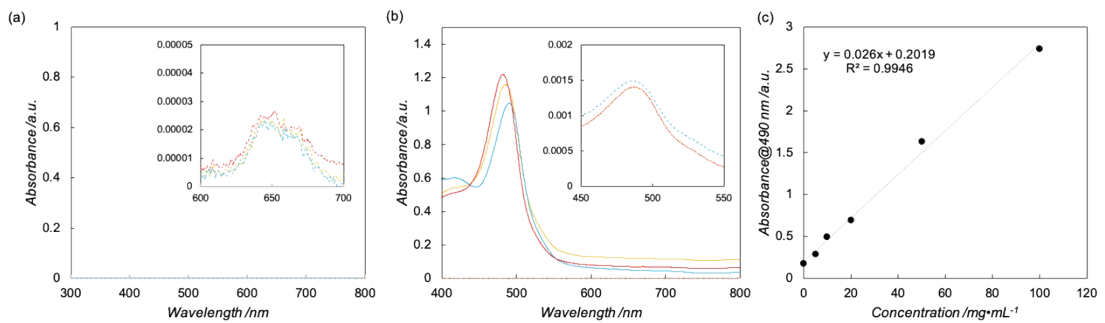
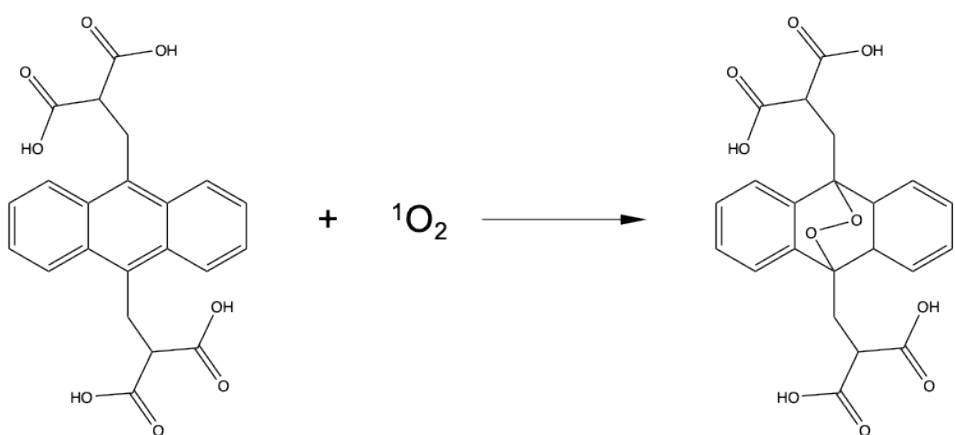


Fig. S10. Homogeneity of Che6P nanogel. (a) UV-Vis spectra of free Che6P polymer isolated by ultracentrifugation (red, Che6P-0.22; yellow, Che6P-0.42; blue, Che6P-0.72). (b) UV-Vis absorption spectra of color products from Che6P before ultracentrifugation (solid line) and after ultracentrifugation (dashed line). Red curve, yellow curve, and blue curve represent Che6P-0.22, Che6P-0.42, and Che6P-0.72, respectively. Inset data represents magnified image. (c) Calibration curve of absorbance at 490 nm for quantification of the amount of free Che6P isolated by ultracentrifugation. Unmodified pullulan was employed to establish the calibration curve.

Table S1. Homogeneity of Che6P nanogel.

	Absorbance@650 nm	Ratio of free Che6P quantified with absorbance@650 nm /%	Phenol-sulfuric acid method, Absorbance@490 nm	Ratio of free Che6P quantified with phenol sulfuric acid method /%
Che6P-0.22	0.000023	0.03	0.0014	0.11
Che6P-0.42	0.000024	0.05	0.0014	0.12
Che6P-0.72	0.000020	0.1	0.0014	0.13

Ratio of free Che6P was calculated as Absorbance of supernatant/Absorbance of Che6P×100.



Scheme S2. Conversion of 9,10-anthracenediyl-bis(methylene)-dimalonic acid (ABDA) to endoperoxide through oxidation with $^1\text{O}_2$.

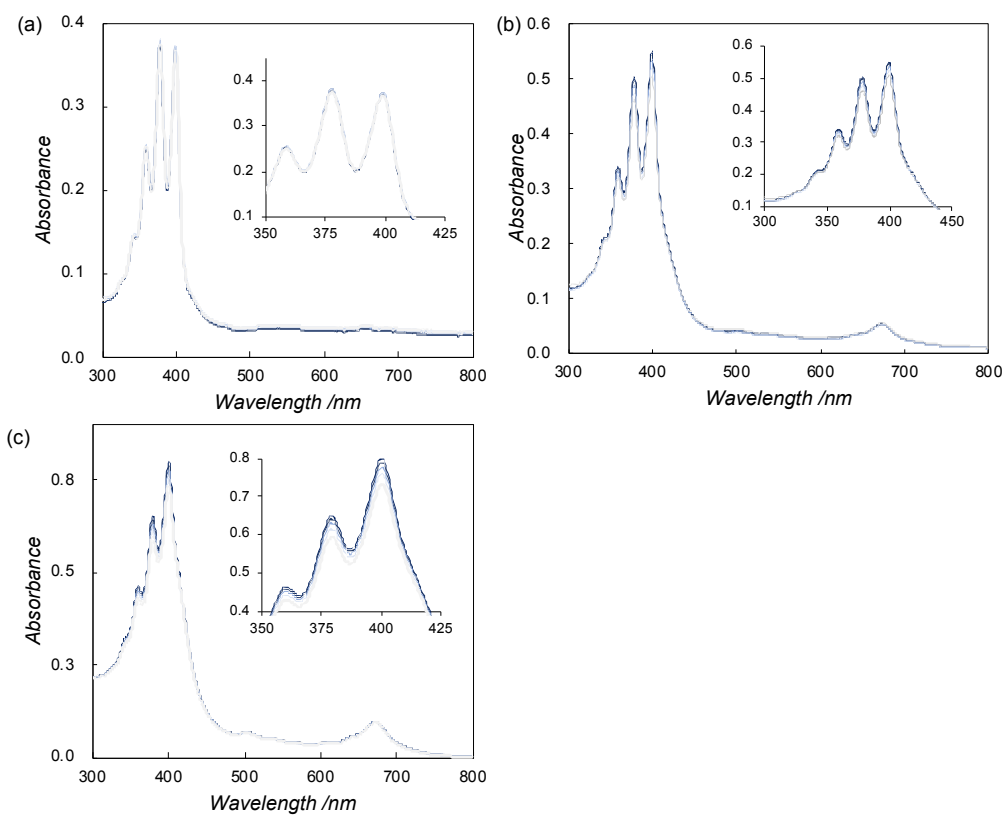


Fig. S11. Representative UV absorption spectra of 9,10-anthracenediyl-bis(methylene)-dimalonic acid (ABDA) bleaching through oxidation with $^1\text{O}_2$ generated using (a) Che6P-0.22, (b) Che6P-0.42, and (c) Che6P-0.72. Polymer concentration was fixed at $1.0 \text{ mg} \cdot \text{mL}^{-1}$.

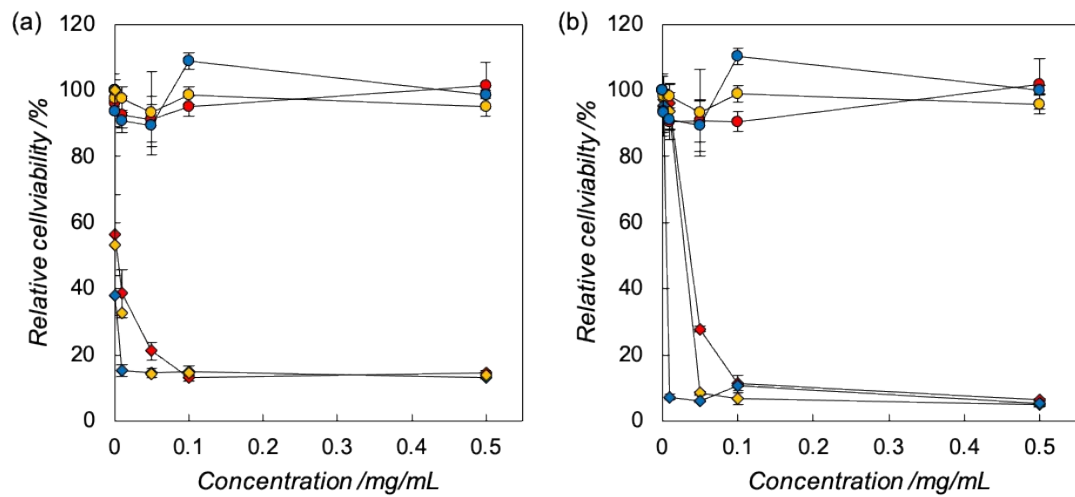


Fig. S12. Photodynamic activity against HeLa (a) and B16BL6 (b) cells. After 24 h incubation with each sample, cells were exposed to light with optimal wavelength for 30 min (red, Che6P-0.22; yellow, Che6P-0.42; blue, Che6P-0.72). Cell viability was evaluated using the WST-8 assay. Data represent mean \pm SD.

Che6P, chlorin e6-bearing pullulan

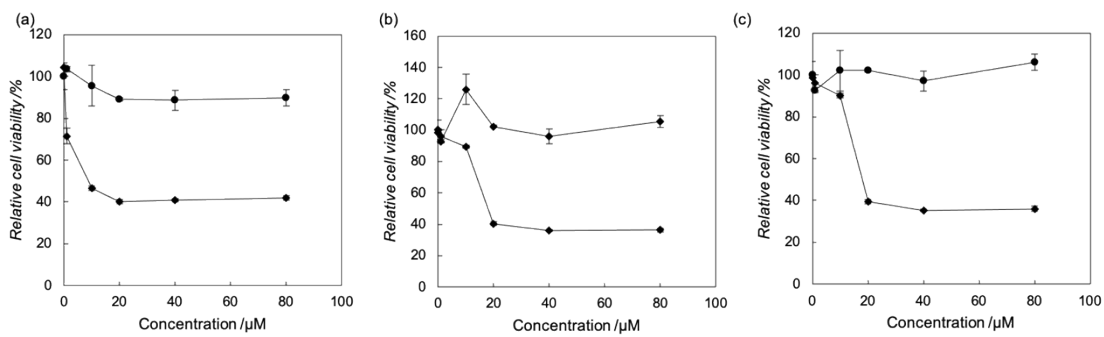


Fig. S13. Photodynamic activity of chlorin e6 against HeLa (a), B16BL6 (b), and colon26 (c) cells. After 24 h incubation with each sample, cells were exposed to light with optimal wavelength for 30 min. Cell viability was evaluated by the WST-8 assay. Data represent mean \pm SD.

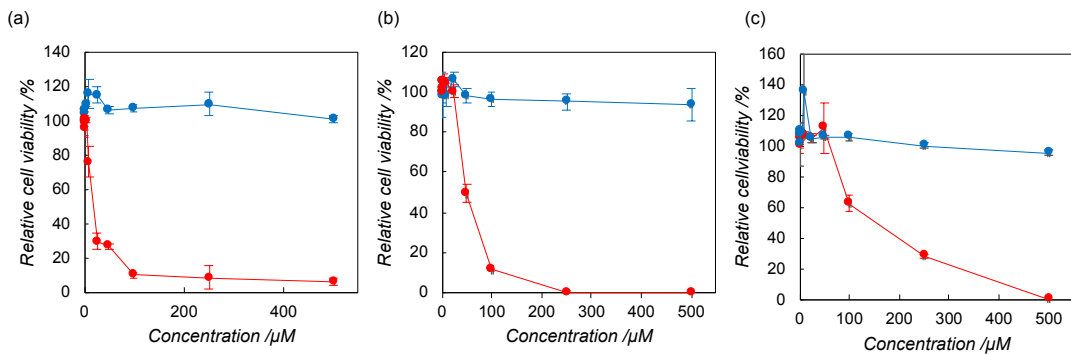
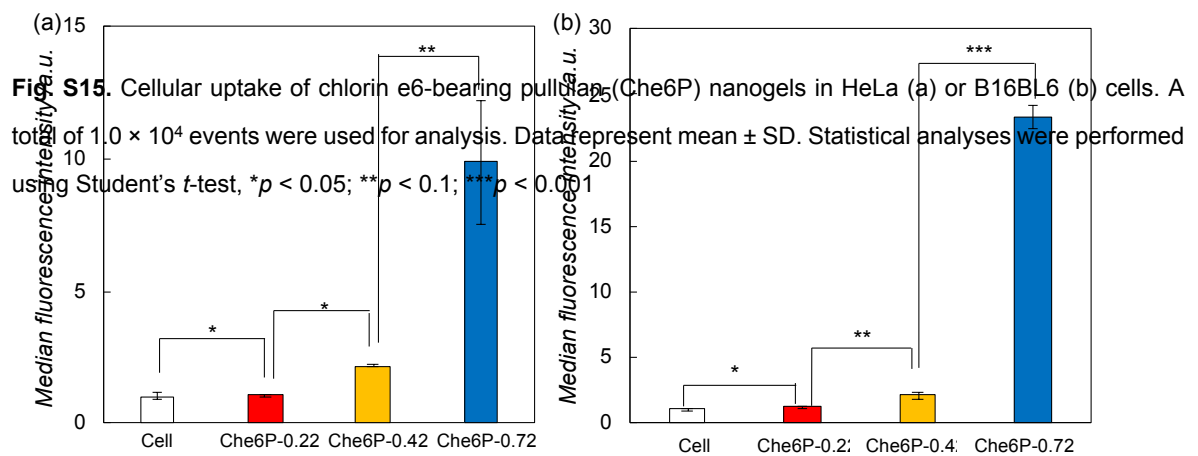


Fig. S14. Photodynamic activity photofrin against HeLa cell (a), B16BL6 cells (b), and colon 26 cells (c). After 24 h incubation with each sample, the cells were exposed to light with optimal wavelength for 30 mins. The cell viability was evaluated by WST-8 assay. Data represents mean \pm SD.



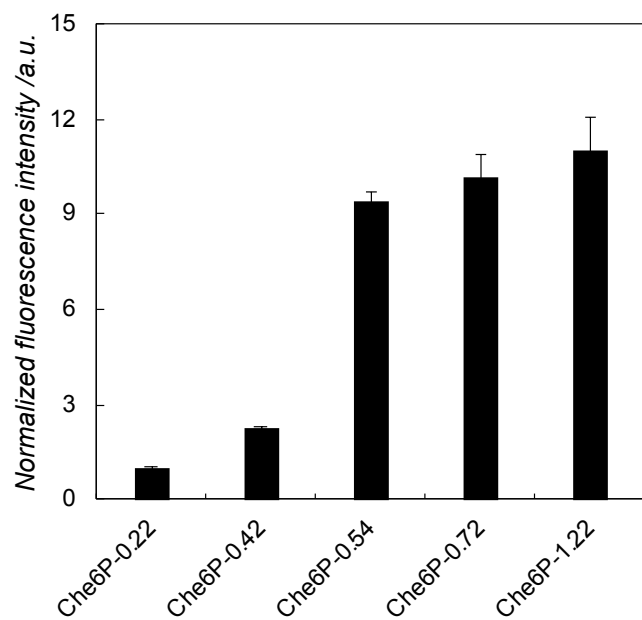


Fig. S16. Cellular uptake amounts of Che6P nanogel toward colon26 cells.

1.0×10^4 events were used for the analysis. Data represents mean \pm SD.

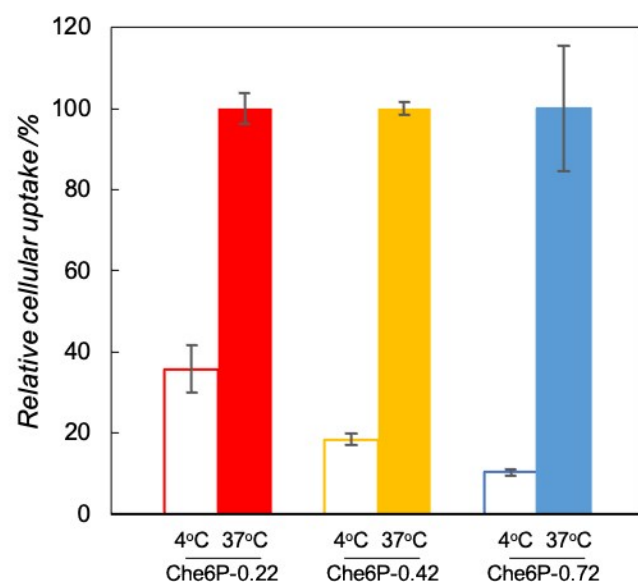


Fig. S17. Endocytosis inhibition assay. Colon26 cells were incubated with chlorin e6-bearing pullulan (Che6P) nanogels at $100 \mu\text{g} \cdot \text{mL}^{-1}$ for 4 h at 4°C (blank) or 37°C (filled). Cells were analyzed by flow cytometry ($N = 3$). Data represent mean \pm SD.

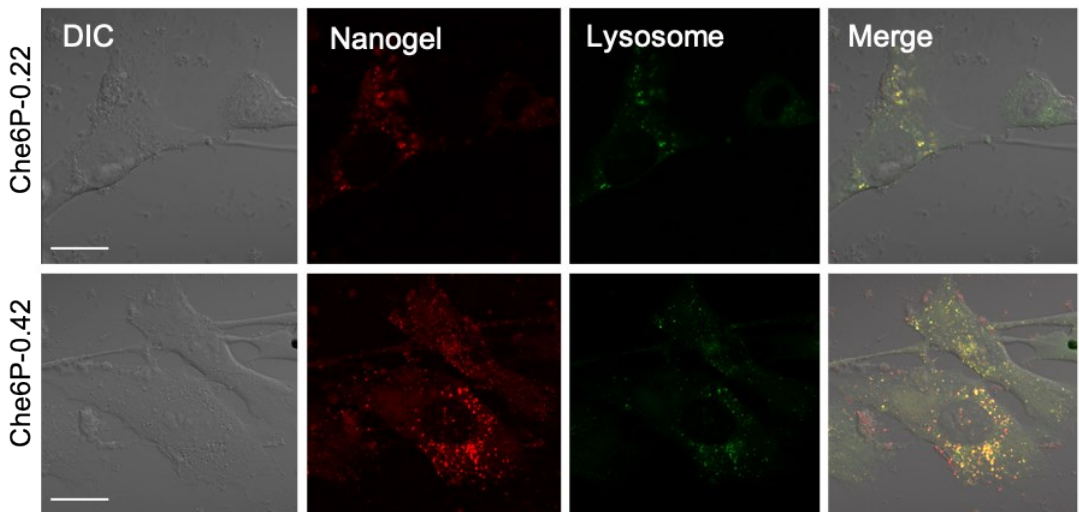


Fig. S18. Subcellular distribution of chlorin e6-bearing pullulan (Che6P) nanogels in colon26 cells. Red, green, and yellow pixels indicate Che6P nanogel, lysosome, and Che6P nanogel–lysosome overlap, respectively. Bar represents 20 μ m.

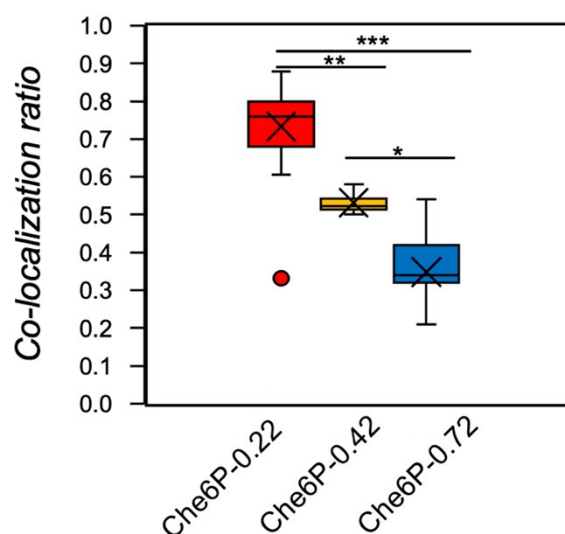


Fig. S19. Co-localization of delivered Che6P with lysosomes. (red, Che6P-0.22; yellow, Che6P-0.42; blue, Che6P-0.72). More than 50 samples were analyzed. Statistical analysis was performed using Student's *t*-test, * p < 0.05; ** p < 0.1; *** p < 0.001.

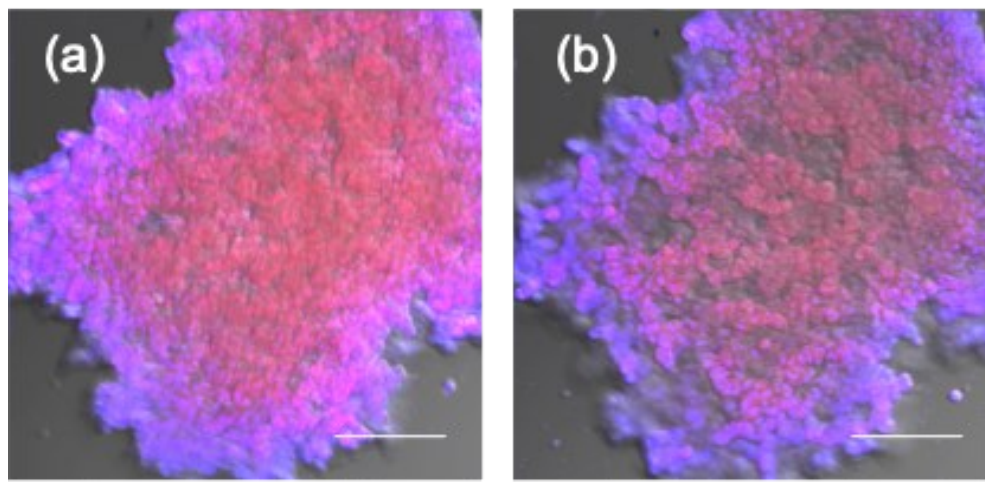


Fig. S20. Distribution of the delivered chlorin e6-bearing pullulan (Che6P) nanogel in colon26 spheroids. Blue, nuclei; red, Che6P nanogel-0.22 (a) and Che6P nanogel-0.42 (b). Bar represents 100 μ m.

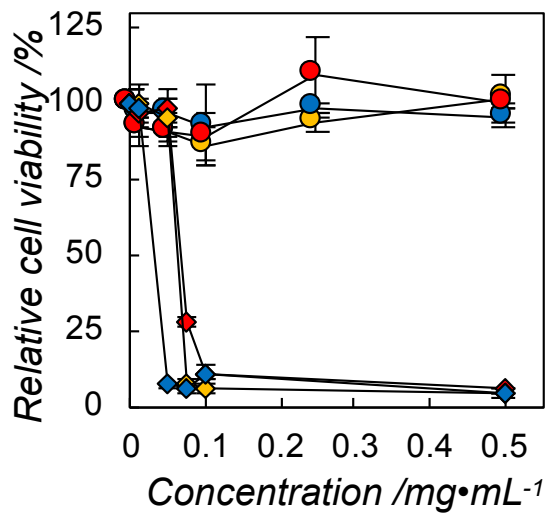


Fig. S21. Photoinduced cytotoxicity against colon26 spheroids using chlorin e6-bearing pullulan (Che6P) nanogels. (circle, non-irradiation control and diamond, photoirradiation; red, Che6P-0.22; yellow, Che6P-0.42; blue, Che6P-0.72)

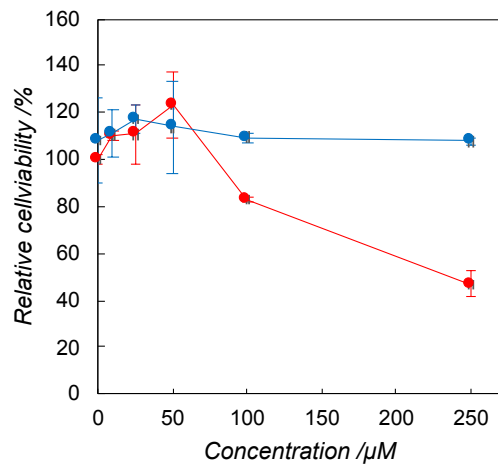


Fig. S22. Photoinduced cytotoxicity against colon26 spheroids using Photofrin (blue, non-irradiation control; red, photoirradiation).

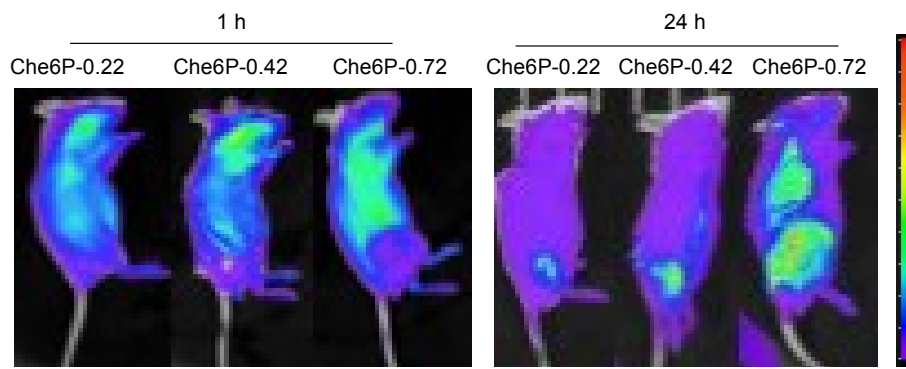


Fig. S23. Tumor accumulation of Che6P nanogel at 1 h (left) and 24 h (right) after administration. Che6P nanogel was administrated toward tumor bearing mice *via* tail vein injection ($1 \text{ mg} \cdot \text{mL}^{-1}$, 100 μL). After administration, tumor accumulation was tracked by optical *in vivo* imaging system.

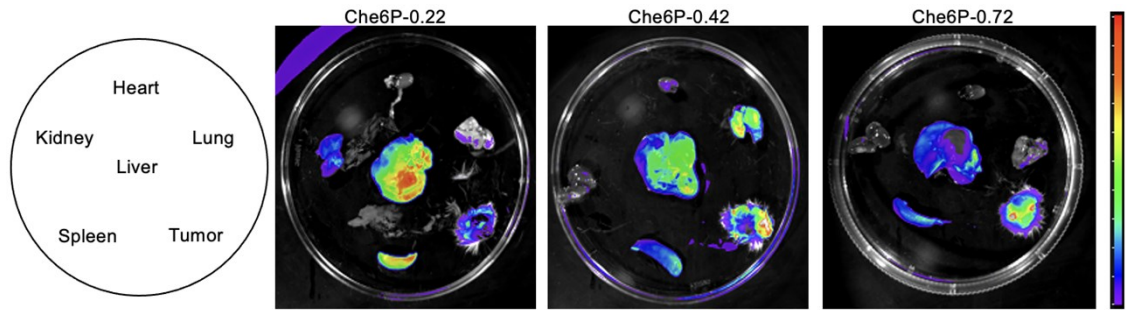


Fig. S24. Biodistribution of Che6P nanogel after 24 h. Che6P nanogel was administrated toward tumor bearing mice *via* tail vein injection ($1 \text{ mg} \cdot \text{mL}^{-1}$, 100 μL). After administration, tumor accumulation was tracked by optical *in vivo* imaging system. After 24 h incubation, organs (tumor, heart, lung, liver, kidney, and spleen) were isolated and the accumulation of Che6P nanogel was visualized by *in vivo* imaging system.

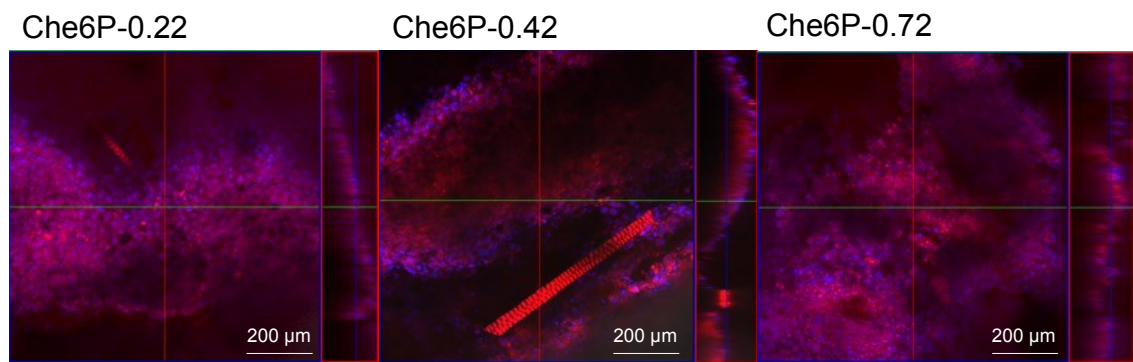


Fig. S25. Intratumoral distribution of Che6P nanogel after 24 h. Che6P nanogel was administrated toward tumor bearing mice *via* tail vein injection ($1 \text{ mg} \cdot \text{mL}^{-1}$, 100 μL). After 24 h incubation, tumor was isolated and the accumulation of Che6P nanogel was visualized by confocal laser scanning microscopy. The cancer cells in tumor tissue was visualized by Hoechst33342 after fixation with 4% paraformaldehyde.